

# Determination of the Helical Screw Sense and Side-Group Chirality of a Synthetic Chiral Polymer from Raman Optical Activity\*\*

Christian Merten, Laurence D. Barron, Lutz Hecht, and Christian Johannessen\*

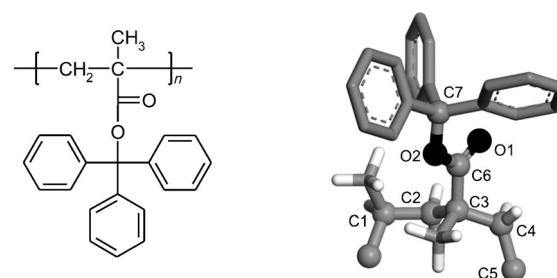
The structures and conformations of the backbones of synthetic polymers exert a major influence on their solution and bulk properties. Among other techniques, infrared and Raman spectroscopy have been extensively used in their study.<sup>[1]</sup> Owing to growing interest in the unique properties of chiral and especially helically chiral polymers, chiroptical methods like electronic circular dichroism (ECD) have also become standard techniques in polymer chemistry.<sup>[2,3]</sup>

Recently the chiroptical versions of infrared and Raman spectroscopy, namely vibrational circular dichroism (VCD) and Raman optical activity (ROA), which measure vibrational optical activity (VOA), have attracted widespread interest.<sup>[4]</sup> While VCD measures the differential absorption of left- and right-circularly polarized infrared radiation by a chiral sample, ROA may be measured either as a small difference in the Raman scattering of right- and left-circularly polarized incident radiation (incident circular polarization (ICP) ROA) or as a small circularly polarized component in the Raman scattered radiation (scattered circular polarization (SCP) ROA).

While several VCD studies of synthetic chiral polymers have been reported,<sup>[5]</sup> ROA has mainly been applied to natural biopolymers. These studies have shown, among other things, that ROA is extremely sensitive to conformations and conformational changes of bio-macromolecules such as polypeptides, carbohydrates, and proteins in solution.<sup>[6]</sup> Apart from a combined experimental and theoretical study of a centrally chiral helical  $\beta$ -peptide,<sup>[7a]</sup> to date all other ROA studies investigating the helical structures of synthetic chiral polymers have been purely theoretical.<sup>[7b-c]</sup> These studies suggest that ROA ought to be very sensitive to helical

structures and capable of providing definitive assignments of the helical screw sense.

Herein we describe the potential of ROA for the structural characterization of synthetic chiral polymers. We report a combined experimental and theoretical study on the helically chiral polymer (+)-poly(trityl methacrylate), referred to as PTrMA. This study completes the VOA analysis of this polymer, which was studied recently by VCD.<sup>[8]</sup> The structure of PTrMA is shown in Scheme 1. The chirality of



**Scheme 1.** Chemical structure of PTrMA (left) and a fragment of the three-dimensional model (right) used in the calculations.

PTrMA arises solely from its one-handed helical backbone and the resulting chiral conformation of the trityl groups and is introduced during chemical synthesis.<sup>[2,9]</sup> The bulky trityl groups prevent the helix from uncoiling and the helical backbone conformation remains intact in solution.

Figure 1a,b shows the solvent- and baseline-corrected experimental Raman and ROA spectra of (+)-PTrMA in chloroform in the spectral region 800–1800  $\text{cm}^{-1}$ . The lower wavenumber region, together with the spectral region 1200–1250  $\text{cm}^{-1}$ , is not shown because of solvent interference. The Raman spectrum (Figure 1a) features three regions with very intense bands assigned to C–H in-plane deformations (1003, 1032, 1156, and 1186  $\text{cm}^{-1}$ ) and C=C stretches (1600  $\text{cm}^{-1}$ ) of the aromatic trityl side groups. Raman bands assigned to backbone vibrations are about one order of magnitude less intense than these intense side-group bands. However, the ROA spectrum (Figure 1b), in which an ROA band is observed for each observed Raman band, does not show significant differences between the intensities of backbone and side-group bands. In fact the average circular intensity difference (CID), the ratio of the ROA to the Raman intensity, in the spectral region 800–1200  $\text{cm}^{-1}$  is approximately  $10^{-3}$ , an order of magnitude larger than that usually observed in typical small chiral molecules. This is partially due to weak Raman bands showing strong ROA.

[\*] Dr. C. Johannessen  
Manchester Interdisciplinary Biocentre, University of Manchester  
131 Princess Street, Manchester M1 7DN (UK)  
E-mail: christian.johannessen@manchester.ac.uk

Dr. C. Merten  
Department of Chemistry, University of Alberta  
Edmonton, AB T6G 2G2 (Canada)  
and  
Fraunhofer Institute for Manufacturing Technology and  
Advanced Materials (IFAM)  
28359 Bremen (Germany)

Prof. Dr. L. D. Barron, Dr. L. Hecht  
WestCHEM, School of Chemistry, University of Glasgow  
Glasgow G12 8QQ (UK)

[\*\*] This work was supported by grants from the UK Engineering and Physical Sciences Research Council.

Supporting information for this article is available on the WWW under <http://dx.doi.org/10.1002/anie.201104345>.

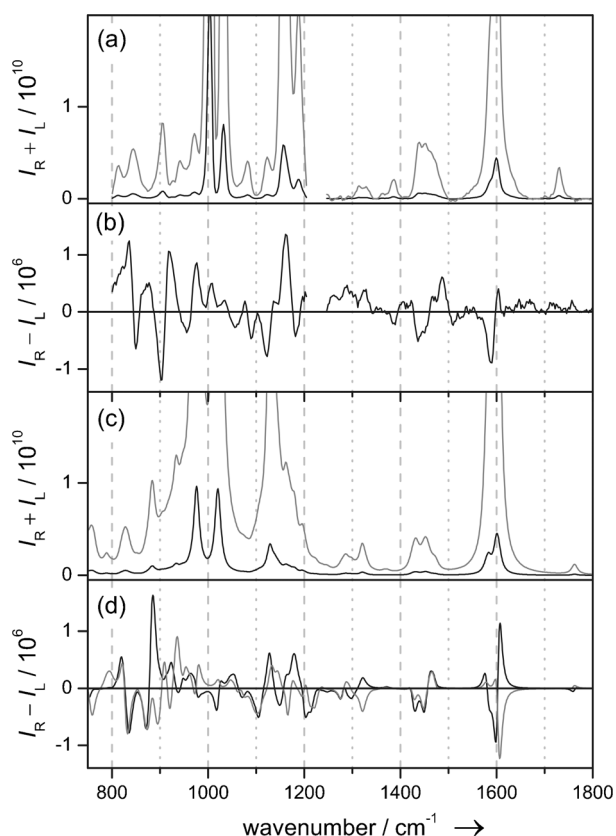


**Figure 1.** Backscattered SCP Raman ( $I_R + I_L$ ) and ROA ( $I_R - I_L$ ) spectra of (+)-PTrMA in chloroform. a,b) Measured Raman and ROA spectra; c) calculated Raman spectrum of a PTrMA 7-mer; d) calculated ROA spectra of a left-handed 7-mer of PTrMA with left-handed (black) and right-handed (gray) trityl propeller structures. The intensity of the predicted spectra was scaled to match that of the experimental spectra. The Raman spectra in gray in (a,c) are multiplied by a factor of 10 to reveal weaker bands more clearly.

Figure 1c,d shows the calculated Raman and ROA spectra of PTrMA, respectively. According to the previous VCD spectroscopic study, the polymer backbone adopts a left-handed helical structure, but no definitive assignment of the handedness of the trityl propeller was obtained.<sup>[8]</sup> Therefore, for the present calculations, two possible structures were considered that consisted of a left-handed helical polymer backbone and either a left- or a right-handed propeller conformation of the trityl groups. The predicted Raman spectra of the two propeller conformations were virtually identical and therefore only one is shown in Figure 1c. The most significant spectral features, for instance the significant differences in Raman intensity between backbone and trityl-group vibrations, are well reproduced in the calculated spectrum. The computed ROA spectra (Figure 1d) show clear differences arising from the two different trityl conformations. The predicted ROA of the PTrMA structure with left-handed trityl propellers agrees very well with the measured ROA pattern. For both propeller conformations the first three bands of the characteristic experimental pattern observed between 800 and 950  $\text{cm}^{-1}$  are reproduced remarkably well, while the remaining bands are predicted with the

correct sign from the left-handed propeller conformation but are inverted in the case of the right-handed propeller conformation. These differences can be explained by normal mode analysis, as the bands detected at 820, 836, and 870  $\text{cm}^{-1}$  can be assigned to backbone  $\text{CH}_2$  rocking modes, while the higher wavenumber bands in this spectral region mainly originate from aromatic C–H deformations. A similar conclusion pertains to the ROA pattern of the C=C stretching vibrations at 1600  $\text{cm}^{-1}$  since the predicted ROA spectrum for the left-handed propeller conformation resembles the experimental pattern while the opposite pattern is found for the right-handed conformation. The ROA bands of the intermediate spectral region are not as strongly affected by the trityl conformation, as the main bands here originate predominantly from backbone vibrations.

The polymer backbone is defined by the two main torsion angles of each unit, C1–C2–C3–C4 and C2–C3–C4–C5 (atomic numbering in Scheme 1); these angles are 165° and –75°, respectively, corresponding to a slightly skewed *trans/gauche*(–) conformation. The small screw angles of each phenyl group of the trityl rings of the left-handed propeller model are all 48°, close to the that of the ideal *gauche*(+) conformation. Based on the normal-mode analysis and comparison of the measured and predicted ROA spectra, we therefore conclude that (+)-PTrMA in chloroform adopts a left-handed helical backbone conformation and a left-handed propeller conformation of the trityl rings.

Calculating the spectra of PTrMA was not as straightforward as for small molecules. Indeed, spectral calculations based on a structural model of a full helical turn (320 atoms) and of a corresponding PTrMA 3-mer as well as of a 7-mer fragment of poly(methyl methacrylate) (PMMA) with locked backbone torsion angles were not successful. Therefore, the method of Cartesian molecular property tensor transfer was applied.<sup>[10]</sup> In this approach a large molecule is split into smaller fragments, for which property tensor calculations (here Raman and ROA intensities) can be calculated at a reasonably high level of theory. The obtained Hessian and Raman/ROA tensors are subsequently transferred back to the initial structure. This procedure allows the prediction of spectra and other properties for larger molecules.

In the present study, the desired large structural model was a 7-mer of PTrMA. The initial point of the tensor transfer was a successfully calculated set of Raman and ROA spectra of a 5-mer of PMMA, in which the relaxation of all backbone torsion angles was restricted by performing geometry optimization with partial optimization in normal modes<sup>[11]</sup> and adopting the input torsion angles from a previous theoretical study on PTrMA.<sup>[12]</sup> Subsequently, the 7-mer of PMMA was generated by tensor transfer; the resulting predicted Raman and ROA spectra are shown in Figure 2a,b. Although the calculated spectra only feature bands originating from the helical backbone, many characteristic patterns observed in the measured ROA spectrum of PTrMA are noticeable.

The next step was the calculation of the Raman and ROA spectra of trityl methacrylate monomers. Therefore, one monomer fragment was cut out of the initial PTrMA model. Calculations were performed for both left- and right-handed propeller conformations of the trityl group of the monomer.

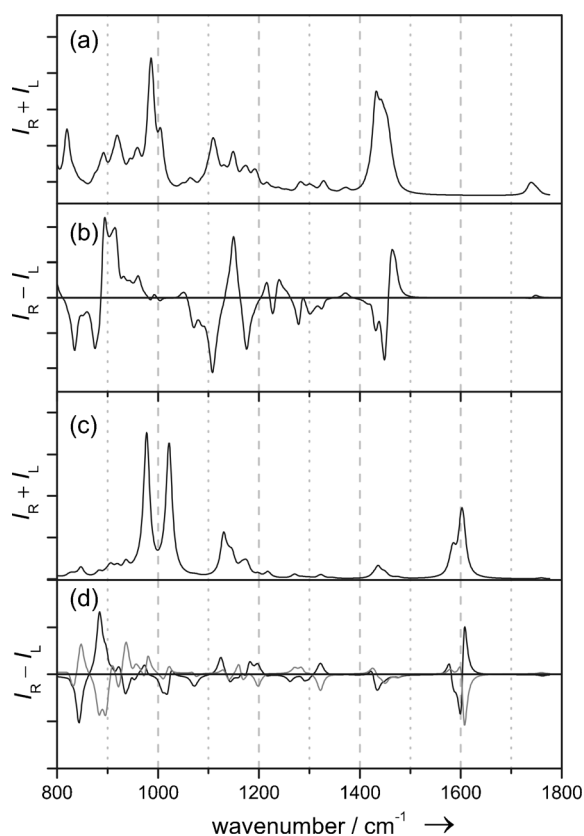


**Figure 2.** Calculated (unscaled) backscattered SCP Raman ( $I_R + I_L$ ) and ROA ( $I_R - I_L$ ) spectra of fragments of (+)-PTrMA used for the tensor transfer. a,b) A 7-mer of PMMA; c,d) a left-handed monomer of PTrMA with left-handed (black) and right-handed (gray) trityl propeller conformations.

The calculations were again carried out with locked backbone torsion angles to ensure that the obtained results could be transferred back to the entire structure. The resulting Raman and ROA spectra are shown in Figure 2c,d. The ROA spectra are not complete mirror images of each other: The two monomer fragments feature identical chiral backbone angles; however, most of the bands originating in vibrations of the phenyl rings show opposite signs. It is noteworthy that the calculated pattern for the C=C stretching vibrations observed at  $1600\text{ cm}^{-1}$ , which are almost unperturbed by mixing with other vibrational coordinates, is conserved upon transfer to the large PTrMA fragment. In the last step, the data of the PMMA 5-mer and of the two monomers were transferred back to the initial PTrMA fragment yielding the two spectra shown in Figure 1c,d.

By comparing the predicted ROA spectra, including the different fragment spectra, with the measured spectrum of PTrMA, we conclude that the ROA spectrum of PTrMA is dominated by bands originating from backbone vibrations, while bands assignable to side-group vibrations are isolated in certain spectral regions. Hence the ROA band patterns are largely determined by the secondary structure of the polymer, that is, the helical backbone, rather than by the local chirality or propeller conformations of the side groups. This conclusion

parallels that previously drawn from theoretical studies of helical peptides and synthetic helicenes.<sup>[13]</sup>

In summary, this combined experimental and theoretical study demonstrates that ROA data can be used to assign both the helical screw sense and the side-group chirality of synthetic chiral polymers with high confidence. A similar objective was achieved previously for natural chiral polymers within a filamentous bacterial virus; in addition to the  $\alpha$ -helical fold of the major coat proteins, ROA also provided the absolute stereochemistry of the tryptophan side chains.<sup>[14]</sup> Extending the application of ROA to the conformational study of synthetic chiral polymers highlights the versatility and sensitivity of the technique.

## Experimental Section

Helical chiral (+)-PTrMA was synthesized according to previously published procedures.<sup>[2,9]</sup> Raman and ROA spectra were measured at ambient temperature in chloroform using the previously described ChiralRAMAN instrument (BioTools, Inc.),<sup>[6a]</sup> which employs the SCP measurement strategy in backscattering. The ROA spectra are presented as intensity differences ( $I_R - I_L$ ) and the parent Raman spectra as intensity sums ( $I_R + I_L$ ), with  $I_R$  and  $I_L$  denoting the Raman-scattered intensities with right- and left-circular polarization states, respectively. The following experimental conditions were employed for the measurement of Raman and ROA spectra: sample concentration  $70\text{ mg mL}^{-1}$ , excitation  $532\text{ nm}$ ; laser power measured at the sample  $\approx 100\text{ mW}$ ; spectral resolution  $\approx 10\text{ cm}^{-1}$ ; acquisition time  $\approx 30\text{ h}$ . The spectrum of the solvent chloroform was subtracted from the parent Raman spectra and all spectra were subsequently smoothed using a second-level Savitzky–Golay filter.

The calculational scheme adopted for the simulation of the polymer structures was based on methods developed by Bouř et al.,<sup>[10,11]</sup> employing the Gaussian 09 program suite<sup>[15]</sup> for gradient, Hessian force field, and ROA intensity tensor calculations. Based on the previous VCD study,<sup>[8]</sup> a model structure of a 5-mer of PMMA in the left-handed helical conformation was optimized, using partial geometry optimization in normal modes and subsequently overlapped to generate a 7-mer PMMA structure. Model structures of the PTrMA monomer in the two propeller conformations were also optimized using the normal-mode methodology to ensure that the torsion angles of the backbone were in agreement with the left-handed helical conformation. The optimized structures were used as input to build the full PTrMA 7-mer models (consisting of 320 atoms) with both propeller conformations, while Hessian force field and ROA intensity tensors were also calculated for each of the smaller model structures. Geometry optimizations and force field calculations were performed at the B3PW91/6-31G(d,p)/in vacuo level, while the ROA intensity tensors ( $532\text{ nm}$  excitation) were evaluated at the HF/rDPS<sup>[16]</sup>/in vacuo level in order to ensure the feasibility of the calculations. After calculation of the property tensors of the PMMA 5-mer and PTrMA monomers, these were transferred onto the PTrMA 7-mer models using the Cartesian tensor transfer approach.<sup>[10]</sup> In the calculated spectra shown the wavenumber axes have been scaled by a factor of 0.96.

Received: June 23, 2011

Published online: September 8, 2011

**Keywords:** chiral polymers · density functional theory · helical chirality · Raman optical activity

- [1] *Vibrational Spectroscopy of Polymers* (Eds.: P. Griffiths, J. Chalmers, N. Everall), Wiley, Chichester, **2007**.
- [2] a) Y. Okamoto, T. Nakano, *Chem. Rev.* **1994**, *94*, 349–372; b) T. Nakano, Y. Okamoto, *Chem. Rev.* **2001**, *101*, 4013–4038.
- [3] a) E. Yashima, K. Maeda, H. Iida, Y. Furusho, K. Nagai, *Chem. Rev.* **2009**, *109*, 6102–6211; b) E. Yashima, *Polym. J.* **2010**, *42*, 3–16.
- [4] a) L. D. Barron, *Molecular Light Scattering and Optical Activity*, Cambridge University Press, Cambridge, **2004**; b) L. D. Barron, A. D. Buckingham, *Chem. Phys. Lett.* **2010**, *492*, 199–213; c) G. Yang, Y. Xu, *Top. Curr. Chem.* **2011**, *298*, 189–236; d) L. A. Nafie, *Vibrational Optical Activity: Principles and Applications*, Wiley, Chichester, **2011**.
- [5] a) H.-Z. Tang, E. R. Garland, B. M. Novak, J. He, P. L. Polavarapu, F. C. Sun, S. S. Sheiko, *Macromolecules* **2007**, *40*, 3575–3580; b) Y. Hase, K. Nagai, H. Iida, K. Maeda, N. Ochi, K. Sawabe, K. Sakajiri, K. Okoshi, E. Yashima, *J. Am. Chem. Soc.* **2009**, *131*, 10719–10732; c) M. Kudo, T. Hanashima, A. Muranaka, H. Sato, M. Uchiyama, I. Azumaya, T. Hirano, H. Kagechika, A. Tanatani, *J. Org. Chem.* **2009**, *74*, 8154–8163.
- [6] a) L. D. Barron, F. Zhu, L. Hecht, G. E. Tranter, N. W. Isaacs, *J. Mol. Struct.* **2007**, *834–836*, 7–16; b) L. D. Barron, *Curr. Opin. Struct. Biol.* **2006**, *16*, 638–643.
- [7] a) J. Kapitán, F. Zhu, L. Hecht, J. Gardiner, D. Seebach, L. D. Barron, *Angew. Chem.* **2008**, *120*, 6492–6494; *Angew. Chem. Int. Ed.* **2008**, *47*, 6392–6394; b) E. Lamparska, V. Liégeois, O. Quinet, B. Champagne, *ChemPhysChem* **2006**, *7*, 2366–2376; c) V. Liégeois, O. Quinet, B. Champagne, *Int. J. Quantum Chem.* **2006**, *106*, 3097–3107; d) V. Liégeois, C. R. Jacob, B. Champagne, M. Reiher, *J. Phys. Chem. A* **2010**, *114*, 7198–7212; e) X. Drooghaag, J. Marchand-Brynaert, B. Champagne, V. Liégeois, *J. Phys. Chem. B* **2010**, *114*, 11753–11760.
- [8] C. Merten, A. Hartwig, *Macromolecules* **2010**, *43*, 8373–8378.
- [9] Y. Okamoto, K. Suzuki, K. Ohta, K. Hatada, H. Yuki, *J. Am. Chem. Soc.* **1979**, *101*, 4763–4765.
- [10] P. Bouř, J. Sopková, L. Bednářová, P. Maloň, T. A. Keiderling, *J. Comput. Chem.* **1997**, *18*, 646–659.
- [11] P. Bouř, T. A. Keiderling, *J. Chem. Phys.* **2002**, *117*, 4126–4132.
- [12] L. Cavallo, P. Corradini, M. Vacatello, *Polym. Commun.* **1989**, *30*, 236–238.
- [13] a) C. Herrmann, K. Ruud, M. Reiher, *ChemPhysChem* **2006**, *7*, 2189–2196; b) V. Liégeois, B. Champagne, *J. Comput. Chem.* **2008**, *30*, 1261–1278.
- [14] a) E. W. Blanch, L. Hecht, L. A. Day, D. M. Pederson, L. D. Barron, *J. Am. Chem. Soc.* **2001**, *123*, 4863–4864; b) C. R. Jacob, S. Luber, M. Reiher, *ChemPhysChem* **2008**, *9*, 2177–2180.
- [15] Gaussian 09, Revision A.1, M. J. Frisch, et al., Gaussian, Inc., Wallingford CT, **2009**.
- [16] G. Zuber, W. Hug, *J. Phys. Chem. A* **2004**, *108*, 2108–2118.